

## Magnetization of superconducting $\text{Hg}_3\text{NbF}_6$ and $\text{Hg}_3\text{TaF}_6$

Thomas W. Krause, T. Olech, P. K. Ummat, and W. R. Datars

*Department of Physics and Astronomy, McMaster University, Hamilton, Ontario, Canada L8S 4M1*

(Received 10 August 1992; revised manuscript received 11 January 1993)

The magnetization of the bulk superconducting transitions of  $\text{Hg}_3\text{NbF}_6$  and  $\text{Hg}_3\text{TaF}_6$  was measured in the temperature range from 0.1 to 1 K and in magnetic fields from 0 to 50 G. Measurements were performed on both samples in the zero-field-cooled (ZFC) and field-cooled (FC) modes. The magnetization was also measured as the sample warmed through its superconducting transition in the same field in which it had been cooled; this was referred to as the return-warming (RW) mode. A large difference in magnitude between the ZFC and FC modes for both samples indicated the presence of multiply connected regions (or type-II superconductivity). Evidence for both samples of the trapping of flux due to inhomogeneities and defects was provided by the hysteresis measured between the FC and RW modes. The observation of excess magnetization above the critical temperature in magnetic fields below 30 G was attributed to a proximity effect between the observed free mercury and the  $\text{Hg}_3\text{NbF}_6$  and  $\text{Hg}_3\text{TaF}_6$  metals. For the average of the data from the three modes, the  $\text{Hg}_3\text{NbF}_6$  sample exhibited a critical field at absolute zero,  $H_c(0)$ , of 150 G and a critical temperature,  $T_c$ , of 0.38 K. The  $\text{Hg}_3\text{TaF}_6$  had a lower  $H_c(0)$  of 60 G, with a  $T_c$  of 0.44 K.

### I. INTRODUCTION

The compounds  $\text{Hg}_3\text{NbF}_6$  and  $\text{Hg}_3\text{TaF}_6$  belong to a family of chain and sheet mercury compounds. They have single sheets of mercury atoms arranged in a hexagonal net between layers of close-packed octahedral ions.<sup>1</sup> In contrast, the chain compounds  $\text{Hg}_{3-\delta}\text{AsF}_6$  and  $\text{Hg}_{3-\delta}\text{SbF}_6$  consist of chains of mercury atoms that are in channels in two mutually perpendicular directions and the mercury-mercury distance is incommensurate with the tetragonal host lattice.<sup>2</sup>

The resistivity of  $\text{Hg}_3\text{TaF}_6$  and  $\text{Hg}_3\text{NbF}_6$  shows a linear temperature dependence from room temperature down to 35 K, below which the temperature dependence has a higher power ( $T^{2.3}$ ) until saturation is reached below 14 K.<sup>3</sup> This temperature dependence is similar to that of common metals but considerably different from that of the chain compounds for which a linear temperature dependence is not observed.

Bulk superconductivity has been established in the  $\text{Hg}_{3-\delta}\text{AsF}_6$  (Refs. 5 and 6) and  $\text{Hg}_{3-\delta}\text{SbF}_6$  (Ref. 7) chain compounds with a critical temperature,  $T_c=0.42$  K and critical fields of 16 and 15 G for  $\text{Hg}_{3-\delta}\text{AsF}_6$  and  $\text{Hg}_{3-\delta}\text{SbF}_6$ , respectively. The sheet compounds,  $\text{Hg}_3\text{NbF}_6$  and  $\text{Hg}_3\text{TaF}_6$ , have not been investigated below 1.4 K, and above this temperature the superconductivity that was reported<sup>4</sup> was not confirmed.<sup>3</sup>

Superconductivity effects which exhibit a small Meissner effect between the bulk transition and 4 K have been observed in the chain compounds<sup>5-7</sup> and have been associated with dispersed isolated regions of mercury trapped within the sample.<sup>8,9</sup> The source of this mercury is extrusion from the compound due to a small contraction of the mercury chains compared to that of the  $\text{AsF}_6$  lattice<sup>10</sup> or due to the presence of minute amounts of oxygen or water vapor.<sup>5</sup> The superconducting effects observed be-

tween the bulk superconducting transition and 4 K were attributed to a proximity effect between extruded free mercury and the  $\text{Hg}_{3-\delta}\text{AsF}_6$  metal.<sup>5</sup>

In this paper, the presence of a bulk superconducting transition at approximately 0.4 K in the  $\text{Hg}_3\text{NbF}_6$  and  $\text{Hg}_3\text{TaF}_6$  sheet compounds is established through the measurement of the temperature dependence of the magnetization in an applied magnetic field. The critical field at absolute zero  $H(0)$  is also estimated. The observation of a free mercury transition, possibly due to mercury extrusion, is used to explain the excess magnetization observed above the bulk superconducting transition. As well, excessive flux trapping in a magnetic field is associated with inhomogeneities and multiply connected regions within the sample.

### II. EXPERIMENTAL PROCEDURE

Each sample was centered in a double-gradient pickup coil system. The four coils consisted of 14 turns each with two center coils wound in the same direction, but in the opposite direction to the two outer coils. The coil system formed one continuous superconducting loop, which matched the impedance of the input coil of a superconducting quantum interference device (SQUID). Measurements were made in a constant magnetic field. The temperature of the sample was controlled with a heater thermally connected to the sample. The magnetization was determined from the SQUID output, while the temperature was measured with a germanium resistance thermometer.

The dilution refrigerator provided 100- $\mu$ W cooling power at 100 mK. The lowest temperature of the sample which was connected thermally with No. 28 cooper wire to the outside of the mixing chamber was 60 mK. The magnetic field was produced by a 3000-turn supercon-

ducting magnet that surrounded the double-gradient pickup coil.

The  $\text{Hg}_3\text{NbF}_6$  sample had dimensions of  $2.3 \times 1.8 \times 1.2 \text{ mm}^3$  with the  $c$  axis parallel to the smallest dimension and a mass of 0.03 g. The dimensions of the  $\text{Hg}_3\text{TaF}_6$  sample were  $1.8 \times 1.6 \times 1.4 \text{ mm}^3$  with the  $c$  axis parallel to the smallest dimension and the mass was 0.027 g. Both samples were mounted and sealed in plastic kelf sample holders in a dry box containing a nitrogen atmosphere. Each was mounted so that the  $c$  axis was parallel to the applied magnetic field. Inspection of each sample after each set of measurements indicated the presence of small amounts of free mercury on the sample surface without major sample decomposition. As well, measurements at 4.2 K indicated a free mercury transition in both the  $\text{Hg}_3\text{NbF}_6$  and  $\text{Hg}_3\text{TaF}_6$  samples.

The data were taken in three modes. In the zero-field-cooled (ZFC) or shielding mode, the sample was first cooled through the transition with no applied magnetic field. A magnetic field applied at the lowest temperature was excluded from the sample by shielding currents, and the data were taken as a function of increasing temperature. In the field-cooled (FC) or Meissner mode, the sample was cooled through the transition in a fixed field while the magnetization was measured. Finally, the sample was warmed through its transition in the same field that it was cooled in and the magnetization was measured. This was the return-warming (RW) mode.

### III. RESULTS

The demagnetization factor was calculated to first order and averaged over the sample volume for each sample. The technique, which was used previously for the chain compound  $\text{Hg}_{3-8}\text{AsF}_6$ ,<sup>5</sup> was based on the equations by Joseph and Schlomann.<sup>11</sup> The demagnetization factor averaged over the sample volume for the  $\text{Hg}_3\text{NbF}_6$  sample was calculated to be 0.46 and that for the  $\text{Hg}_3\text{TaF}_6$  sample was 0.38.  $T_c$  was defined as the temperature at the midpoint of the magnetization transition. The results for the critical field as a function of temperature are presented after adjusting the internal field by the demagnetization factor to describe a sample with a demagnetization factor of zero.

#### A. $\text{Hg}_3\text{NbF}_6$

Magnetization as a function of temperature in the ZFC and FC modes is shown for the  $\text{Hg}_3\text{NbF}_6$  sample in an applied field of 19 G in Fig. 1. The magnitude of the change of the magnetization in the ZFC mode is 11 times larger than that for the FC mode. This ratio is 16 in a field of 4 G.

Hysteresis between the FC and RW curves in an applied field of 19 G is exhibited in a plot of magnetization as a function of temperature for the  $\text{Hg}_3\text{NbF}_6$  sample in Fig. 2. Arrows indicate the directions in which the data were taken. The magnitudes of the FC and RW curves are comparable. The hysteresis takes the form of a difference in temperature between the FC and RW modes at the same level of magnetization. It was shown that it

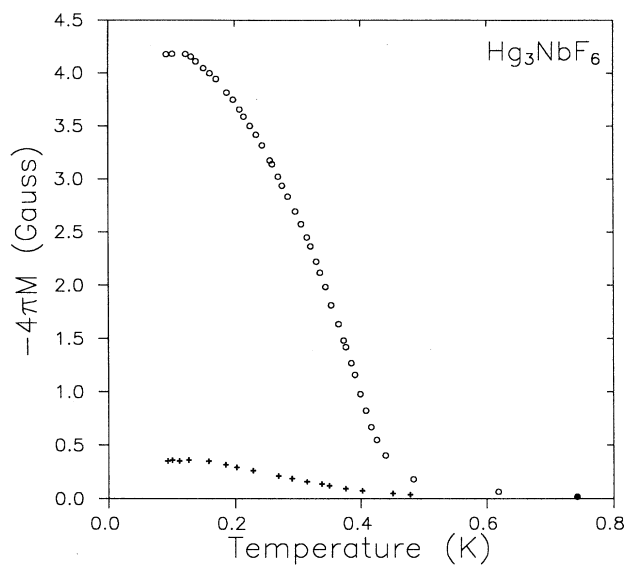


FIG. 1. Magnetization as a function of temperature for the ZFC (○) and the FC (+) modes for the  $\text{Hg}_3\text{NbF}_6$  sample in a 19-G applied field.

was not from a thermal lag between the sample and thermometer.

A plot of the critical field as a function of temperature for the  $\text{Hg}_3\text{NbF}_6$  sample with zero demagnetization factor is shown in Fig. 3. The temperature of the critical field was defined as the temperature at the midpoint of the magnetization curve for that particular field applied to the sample. The value of the temperature at the mid-

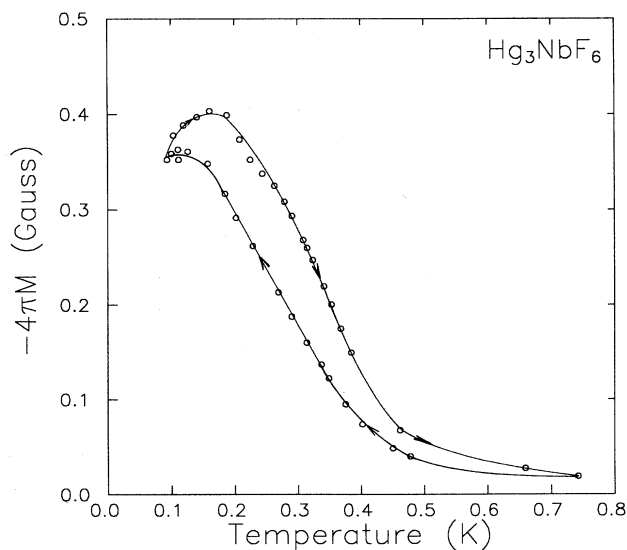


FIG. 2. Magnetization as a function of temperature for the  $\text{Hg}_3\text{NbF}_6$  sample for the FC and RW modes in a 19-G applied field. Arrows indicate the directions in which the data were taken.

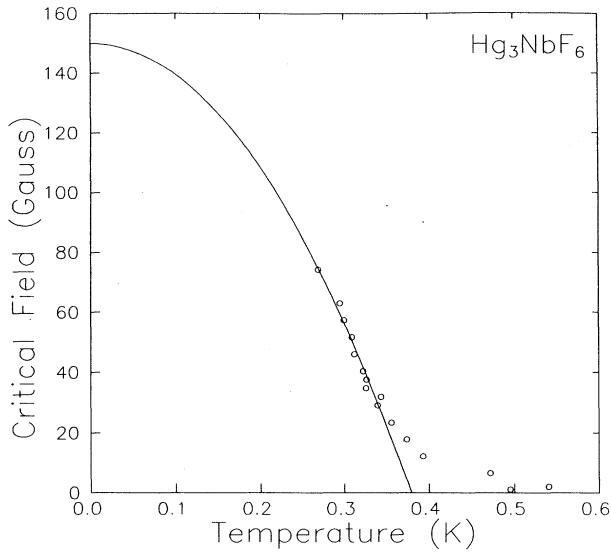


FIG. 3. Critical field as a function of temperature for the  $\text{Hg}_3\text{NbF}_6$  sample. The solid line is a fit of Eq. (1) for fields greater than 30 G.

point of the magnetization curve depends on the mode of taking data because of the hysteresis between the FC and RW curves. Therefore, the temperature for the critical field was taken as the average of the midpoint temperatures of the ZFC, FC, and RW modes. The critical field as a function of temperature curve was fit with the empirical formula

$$H_c(T) = H_c(0)[1 - (T/T_c)^2], \quad (1)$$

above critical fields of 30 G, since below this field the magnetization extends to higher temperatures from the proximity effect. The fit parameters  $H_c(0)$  and  $T_c$  are 150 G and 0.38 K, respectively. The value of  $H_c(0) = 150$  G lies between that obtained from the FC mode,  $H_c(0) = 160$  G, and that obtained from the RW mode,  $H_c(0) = 140$  G. The value of  $T_c = 0.38$  K is also the average of the  $T_c$ 's obtained from fitting each of the ZFC, FC, and RW modes separately with a standard deviation of 0.03 K.

The average magnetization between the ZFC and FC modes as a function of applied field at 0.1 K for the  $\text{Hg}_3\text{NbF}_6$  sample is shown in Fig. 4. The magnetization between 0 and 16 G was fit with a straight line. This was used to calibrate the magnetization with the slope taken as  $1/(1-n)$ , where  $n$  was the demagnetization factor.<sup>12</sup> Between 20 and 35 G the magnetization decreased linearly before reducing more slowly as a function of field. The magnetization was not zero in the maximum applied field of 48 G.

### B. $\text{Hg}_3\text{TaF}_6$

Magnetization as a function of temperature in the ZFC and FC modes is shown for the  $\text{Hg}_3\text{TaF}_6$  sample in an applied field of 1.8 G in Fig. 5. The magnitude of the ZFC signal is seven times larger than the FC signal.

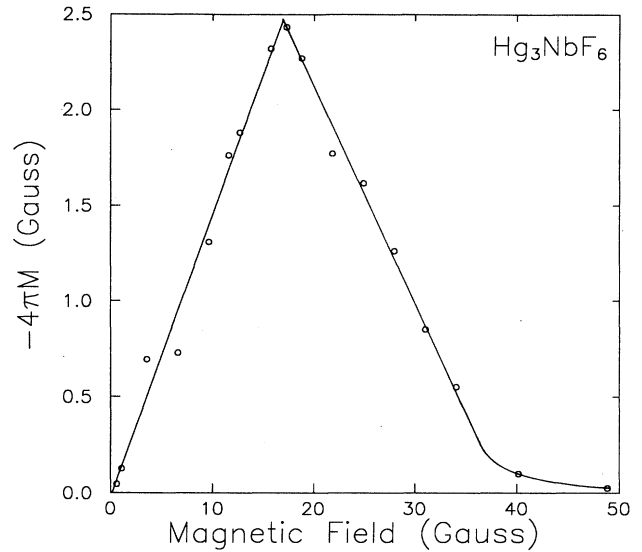


FIG. 4. Magnetization as a function of applied field for the  $\text{Hg}_3\text{NbF}_6$  sample at 0.1 K. Between 0 and 16 G the data were fitted with a straight line. The solid curve above 16 G is a guide to the eye.

Hysteresis is shown for the  $\text{Hg}_3\text{TaF}_6$  sample between the FC and RW curves in an applied field of 20 G in Fig. 6. Arrows indicate the direction in which the data were taken. As in the  $\text{Hg}_3\text{NbF}_6$  sample, the total magnitude of the FC and RW curves is the same. Again the hysteresis is demonstrated by a difference in temperature at equivalent levels of magnetization between the FC and RW modes.

A plot of critical field as a function of temperature for

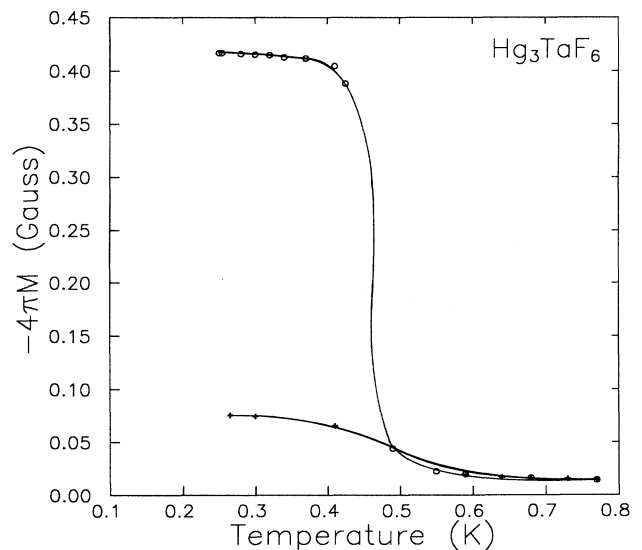


FIG. 5. Magnetization as a function of temperature for the ZFC (○) and the FC (+) modes for the  $\text{Hg}_3\text{TaF}_6$  sample in a 1.8-G applied field.

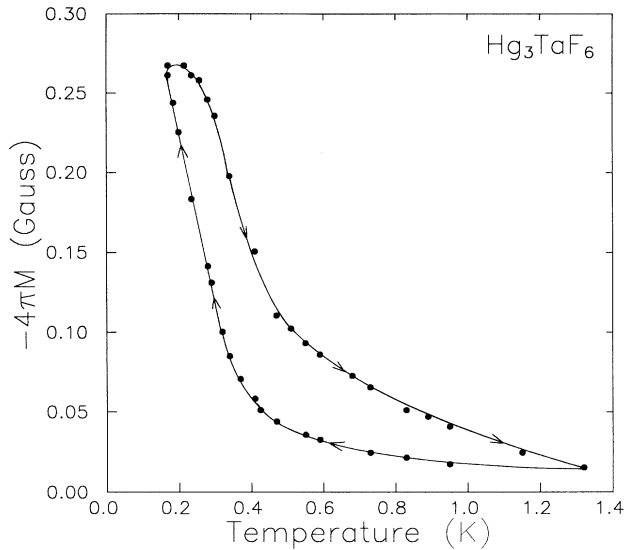


FIG. 6. Magnetization as a function of temperature for the  $\text{Hg}_3\text{TaF}_6$  sample for the FC and RW modes in a 20-G field. Arrows indicate the directions in which the data were taken.

the  $\text{Hg}_3\text{TaF}_6$  sample with zero demagnetization factor is shown in Fig. 7. The temperature for the critical field is again the average midpoint temperature of the ZFC, FC, and RW modes. The curve has been fitted with the empirical formula Eq. (1) above critical fields of 10 G, because of the tail extension to higher temperatures of the critical field in fields below 10 G. The fit parameters are  $H_c(0)=60$  G and  $T_c=0.44\pm 0.04$  K with uncertainties estimated from separate fits to the FC and RW curves. Again excess magnetization in the form of higher mid-

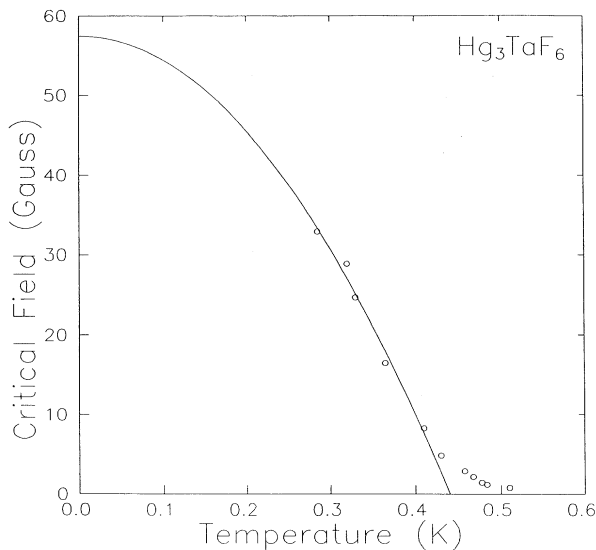


FIG. 7. Critical field as a function of temperature for the  $\text{Hg}_3\text{TaF}_6$  sample. The solid line is a fit of Eq. (1) for fields greater than 10 G.

point temperatures was observed for all three modes for fields below 10 G.

#### IV. DISCUSSION

The difference in the total change of magnetization between the FC and ZFC modes was greater in the sheet compounds measured in this experiment than was observed in similar measurements of the  $\text{Hg}_{3-\delta}\text{AsF}_6$  compound.<sup>5</sup> Likewise, the hysteresis between the FC and RW curves was greater.<sup>13</sup> However, in measurements of the  $\text{Hg}_{3-\delta}\text{AsF}_6$  compound, hysteresis was observed to increase with increased sample degradation and an increased free mercury signal.<sup>13</sup> The amount of excess magnetization above  $T_c$  in low fields was also greater in the two sheet compounds investigated here when compared to results for the chain compounds.<sup>5,7</sup>

The presence of hysteresis and the large differences between the ZFC and FC magnetization signals complicate the evaluation of the critical field as a function of temperature. It is clear from Figs. 2 and 6 that hysteresis affects the value of the midpoint temperature and, therefore, the evaluated critical field. Taking the reversible magnetization curve to lie between the FC, RW, and ZFC curves, an average of the midpoint temperatures taken in these three modes was made for each sample to obtain an estimate of the reversible magnetization curve. This provided an estimate with uncertainty of the critical field at absolute zero,  $H_c(0)$  and critical temperature in zero field  $T_c$  for the two samples. For the  $\text{Hg}_3\text{NbF}_6$  sample,  $H_c(0)=150\pm 10$  G and  $T_c=0.38\pm 0.03$  K and for the  $\text{Hg}_3\text{TaF}_6$ ,  $H_c(0)=60$  G and  $T_c=0.44\pm 0.04$  K. The  $\text{Hg}_3\text{NbF}_6$  sample has a lower  $T_c$  but a higher  $H_c(0)$ .

The magnetization curve of  $\text{Hg}_3\text{NbF}_6$  in Fig. 4 suggests characteristics of a type-I superconductor,<sup>15</sup> although the apparent results may have been modified by the averaging of the FC and ZFC signals. The finite declining slope of the magnetization curve in Fig. 4 may be explained as being due to the finite demagnetization factor of the sample.<sup>14</sup> The small tail observed at the end of the demagnetization curve we attribute to the presence of a proximity effect between free mercury and the sheet compound itself, an effect suggested previously for the chain compounds.<sup>5</sup>

The critical temperature of the bulk superconducting transition of the  $\text{Hg}_{3-\delta}\text{AsF}_6$  and  $\text{Hg}_{3-\delta}\text{SbF}_6$  mercury chain compounds of 0.42 K is similar to those of the mercury sheet compounds  $\text{Hg}_3\text{NbF}_6$  and  $\text{Hg}_3\text{TaF}_6$ . While the chain compounds have critical fields of about 15 G,<sup>5,7</sup> the sheet compounds have critical fields that are factors of 10 and 4 larger for  $\text{Hg}_3\text{NbF}_6$  and  $\text{Hg}_3\text{TaF}_6$ , respectively. Although the stoichiometric ratios in the sheet and chain compounds are similar, their structures are quite different.<sup>1,2</sup> We associate the differences in  $H_c$  between the sheet and chain compounds as being due to structure and the substitution of the elements Nb and Ta for As and Sb.

One source of hysteresis and large difference in the magnitude between the ZFC and FC magnetization signals is attributed to inhomogeneities, defects, and multiply connected regions.<sup>14</sup> Multiply connected regions are

formed from loops of superconducting material that shield normal or nonsuperconducting regions. In the ZFC mode normal regions are shielded by multiply connected superconducting regions that keep flux from penetrating and, therefore, make the apparent superconducting volume larger than it really is. In the FC mode these regions trap flux within the sample, reducing the total magnetization signal. Likewise, defects and inhomogeneities pin flux and keep it from moving easily either in or out of the sample.<sup>14</sup> The size of the coherence length may determine how easily superconducting-normal (SN) boundaries may move through the sample. Materials with larger coherence lengths have more diffuse SN boundaries and are not as easily pinned.<sup>14</sup> In the mercury sheet and chain compounds a source of such multiply connected regions, inhomogeneities, and defects may be the extrusion of free mercury and its dispersion within the sample<sup>8,9</sup> or on the surface.<sup>10</sup>

The sheet compounds may also have a greater type-II superconducting nature than the chain compounds. This could explain the hysteresis, large differences in magnitude between the FC and ZFC magnetization signals, and the higher critical fields measured in these materials when compared to the critical fields measured in the chain compounds. If type-II superconductivity is present in the sheet compounds then the interpretation of the averaged FC and ZFC signal in Fig. 4 as being due to type-I superconductivity may be a result of the low temperature (0.1 K) at which the data were analyzed.

The differences between the chain and the sheet compounds in hysteresis and the ratio of the ZFC to the FC total change in magnetization may be due to: (a) an increased number of multiply connected regions, defects, and inhomogeneities in the sheet compounds due to increased sample degradation, and/or (b) a greater type-II superconducting nature.

The observation of excess magnetization above  $T_c$  is in agreement with similar observations made with the  $\text{Hg}_{3-\delta}\text{AsF}_6$  and  $\text{Hg}_{3-\delta}\text{SbF}_6$  compounds.<sup>5,7-9</sup> The excess magnetization has been attributed to a proximity effect between free mercury interspersed throughout the metal and the  $\text{Hg}_{3-\delta}\text{AsF}_6$  metal itself.<sup>5</sup> This proximity effect is removed when a "breakdown" field is reached where the entrance of domain walls separates the normal and superconducting regions.<sup>15</sup> If the extension to higher tempera-

tures of the critical field in small fields is associated with such a proximity effect, the fields in both samples where the tails disappear into the transition may be due to such a breakdown field. This breakdown field is about 30 G for the  $\text{Hg}_3\text{NbF}_6$  sample and 10 G for the  $\text{Hg}_3\text{TaF}_6$  sample. The larger extension of the magnetization to higher temperatures in small field than that observed in the  $\text{Hg}_{3-\delta}\text{AsF}_6$  may again be due possibly to more free mercury dispersed throughout the volume of the measured samples. This is in agreement with observations made with the  $\text{Hg}_{3-\delta}\text{AsF}_6$  chain system where the amount of excess magnetization was found to be associated with the amount of free mercury in the system.<sup>9</sup>

## V. CONCLUSION

The mercury sheet compounds,  $\text{Hg}_3\text{NbF}_6$  and  $\text{Hg}_3\text{TaF}_6$ , exhibited superconducting transitions at a temperature of approximately 0.4 K. The difference in the total change in magnetization between the ZFC and FC modes was attributed to the presence of inhomogeneities in the form of multiply connected regions. These regions of normal material, surrounded by bulk superconducting material, may have been the result of extruded elemental mercury that was observed in the magnetization at 4.2 K. The presence of inhomogeneities was also supported by the considerable hysteresis observed between the field-cooled and return-warming curves taken in fixed magnetic field. The possibility that these effects may be due to the presence of type-II superconductivity was also considered. The observation of excess magnetization above the bulk superconducting transition of both samples was attributed to a proximity effect between the  $\text{Hg}_3\text{NbF}_6$  and  $\text{Hg}_3\text{TaF}_6$  compounds and the superconducting free mercury. Estimates of the critical field at absolute zero and the critical temperature in zero field were made.  $H_c(0)$  for  $\text{Hg}_3\text{NbF}_6$  was determined to be  $150 \pm 10$  G and  $T_c$  was determined as  $0.38 \pm 0.03$  K. For  $\text{Hg}_3\text{TaF}_6$ ,  $H_c(0) = 60$  G and  $T_c = 0.44 \pm 0.04$  K.

## ACKNOWLEDGMENT

The research was supported by the Natural Sciences and Engineering Research Council of Canada.

<sup>1</sup>I. D. Brown, R. J. Gillespie, K. R. Morgan, Z. Tun, and P. K. Ummat, *Inorg. Chem.* **23**, 4506 (1984).

<sup>2</sup>I. D. Brown, B. D. Cutforth, C. G. Davies, R. J. Gillespie, P. R. Ireland, and J. E. Vekris, *Can. J. Chem.* **52**, 791 (1974).

<sup>3</sup>W. R. Datars, F. S. Razavi, R. J. Gillespie, and P. Ummat, *Philos. Trans. R. Soc. London Ser. A* **314**, 115 (1985).

<sup>4</sup>W. R. Datars, K. R. Morgan, and R. J. Gillespie *Phys. Rev. B* **28**, 5049 (1983).

<sup>5</sup>T. W. Krause, P. K. Ummat, and W. R. Datars, *Phys. Rev. B* **45**, 4836 (1992).

<sup>6</sup>F. Gross, H. Veith, K. Andres, M. Weger, and A. G. McDiarmid, *Phys. Rev. B* **34**, 3503 (1986).

<sup>7</sup>P. A. Laroche and W. R. Datars, *Phys. Rev. B* **35**, 3170 (1987).

<sup>8</sup>J. E. Schirber, A. J. Heeger, and P. J. Nigrey, *Phys. Rev. B* **26**,

6291 (1982).

<sup>9</sup>E. Batalla and W. R. Datars, *Solid State Commun.* **45**, 225 (1983).

<sup>10</sup>W. R. Datars, A. van Schyndel, J. S. Lass, D. Chartier, and R. J. Gillespie, *Phys. Rev. Lett.* **40**, 1184 (1978).

<sup>11</sup>R. I. Joseph and E. Schlomann, *J. Appl. Phys.* **36**, 1579 (1965).

<sup>12</sup>D. Shoenberg, *Superconductivity* (Cambridge University Press, London, 1952), p. 22.

<sup>13</sup>T. W. Krause, M. Sc. thesis, McMaster University, 1989 (unpublished).

<sup>14</sup>J. D. Livingston and H. W. Schadler, *Prog. Mater. Sci.* **12**, 185 (1963).

<sup>15</sup>P. G. de Gennes, in *Quantum Fluids*, edited by D. F. Brewer (North-Holland, Amsterdam, 1966), p. 26.